Advanced Materials Research *Online: 2013-05-27*
ISSN: 1662-8985, Vol. 699, pp 822-828
doi:10.4028/www.scientific.net/AMR.699.822

Computational Fluid Dynamics Modeling of Palm Fruit Pyrolysis in a Fast Fluidized Bed Reactor

P. L. Mtui

College of Engineering and Technology, University of Dar es Salaam, P. O. Box 35131
Dar es Salaam, Tanzania
Email: plmtui@yahoo.com

Keywords: CFD, palm fruit, pyrolysis, fluidized bed, reactor

Abstract. The palm fruit biomass is introduced into the pyrolysis reactor bed and the transport equations for heat, mass and momentum transfer are solved using computational fluid dynamics (CFD) technique. The Eulerian-Eulerian approach is employed to model fluidizing behavior of the sand for an externally heated reactor prior to the introduction of the biomass. The particle motion in the reactor is computed using the drag laws which depend on the local volume fraction of each phase. Heat transfer from the fluidized bed to the biomass particles together with the pyrolysis reactions were simulated by Fluent CFD code through user-defined function (UDF). Spontaneous production of pyrolysis oil, char and non-condensable gases (NCG) confirm the observation widely reported in literature. The computer model can potentially be used to assess other candidate biomass sources also to assist design of optimized pyrolysis reactors.

Introduction

Biomass pyrolysis for bio-refinery has the potential to replace a substantial amount of fossil fuel utilization. Thermochemical conversion of biomass (i.e., combustion, pyrolysis, or gasification) is receiving increasing interest as a method for production of renewable energy and fuels. Fast pyrolysis is a rapid decomposition of organic matter in the absence of oxygen to produces solid (char), liquid (pyrolysis oil), and gas (non-condensable gases, NCG). The liquid comprises the largest product fraction when pyrolysis is performed at 500 °C. Direct combustion of bio-oils as a substitute for heavy-fuel oil in boilers and gas turbines have been demonstrated [1] For bio-oil to be refined into usable transportation fuel, biorefinery (upgrading) of bio-oil to decrease its oxygen content is required [2]. However, for biorefinery to compete with fossil fuels, it requires a large economics of scale therefore posing logistical challenges for biomass cultivation, harvest and transportation to the biorefinery location. Further, the design of biomass pyrolysis reactor is a challenge that must be addressed for any meaningful production of bio-oil for commercial applications. A key feature of fast pyrolysis is the need to separate the by-product char from the vapours as quickly and as completely as possible as char in the vapours can significantly reduce yields if not efficiently removed.
Recently, extensive research has been conducted in the renewable energy sources in an attempt to understand the major factors that affecting biomass fast pyrolysis. Fluidized beds are the most commonly employed type of reactor for achieving fast pyrolysis of biomass for bio-oil production. There are a number of advantages for this choice, in particular, fast heat transfer and good temperature control. Fluidized beds are very complex systems, however, the design and scale up is mostly based on empirical relationships in a pilot plant work. Advances in computing capabilities and numerical methods have allowed a more fundamental treatment of fluidized bed modeling using computational fluid dynamics (CFD). Most of the computational research interest has been focused on the simulation of the fluidized bed hydrodynamics, of multiphase flows using the Eulerian-Eulerian for non-reactive fluidized beds [3, 4] and chemically reactive flows with heat transfer. The use of CFD to improve design and performance prediction of fluidized beds has been extended to consider separation of char from fluidizing sand and to evaluate the role of reactor geometry in achieving phase separation as effectively as possible [5].

The scope of the present simulation is to determine the heat and momentum transport inside the reactor and the chemical reactions of the palm fruit biomass particle. The model combines the bed hydrodynamics and fast pyrolysis process in a using CFD FLUENT 12 computer code. The model provides a good insight to the heat and mass transfer in fast pyrolysis, and their intricate interaction with reaction kinetics and phase transition phenomena.

Process Description

The cylindrical-shape fast pyrolysis lab scale reactor is illustrated in Figure 1 whose overall length and diameter are 50 cm and 7.5 cm, respectively. The reactor is filled with 180 microns sand particles so that the static height is 12.7 cm. The reactor walls are electrically heated to maintain the reactor temperature at 500^0 C. Biomass particles (100 microns) are introduced into the reactor at 5 kg/hr. Nitrogen flows through a perforated plate at the bottom of the reactor at a velocity of 0.23m/s. The reactor design specifications and operating conditions are discussed by Boateng [6]

Computational Model

The equations of motion for multiphase flow that describe the hydrodynamics of the fluidized bed are solved by the FLUENT code. The Eulerian-Eulerian equations for the conservation of mass, momentum and energy are solved for the continuum and dispersed phases, respectively. The phases are able to interpenetrate and the sum of all the volume mass fractions in each computational cell sums up to one. Besides the traditional terms of a momentum transport equation, the Eulerian-Eulerian equations contain terms to account for interphase forces modeled through the interphase exchange coefficients. Since the Eulerian multiphase model accounts separately for the momentum of each phase, it is able to capture most of the complex physics involved in the multiphase flow problems. In Eulerian multiphase model only the pressure field variable is shared by all the phases. CFD models of the thermochemical processes include description of fluid flow, heat and mass transfer, and chemical reactions. The computational expense is higher when using the Eulerian multiphase model, especially when more than 2 phases are considered.

Conservation of mass for phase q :

For the Eulerian multiphase conservation laws, consider discrete secondary phase p and continuum primary phase q, are given in equations (1) through (4). Note that only phase q equations are presented since phase p follows similar mathematical formulation.

$$\frac{\partial}{\partial t}\alpha_q \rho_q + \nabla \cdot \left(\alpha_q \rho_q \vec{u}_q\right) = \sum_{q=1}^{n} \dot{m}_{pq} \qquad \text{(Eq. 1)}$$

where, the term on the right hand side represents mass transfer.

Conservation of momentum for phase q :

Forces acting in gas–solid fluidized beds consist of the viscous force, the solids pressure, the body force, the static pressure force and the inter-phase force which couples of gas and solid momentum equations through drag forces [10].

$$\frac{\partial}{\partial t}\left(\alpha_q \rho_q \vec{u}_q\right) + \nabla \cdot \left(\alpha_q \rho_q \vec{u}_q \vec{u}_q\right) = -\alpha_q \nabla p + \nabla \cdot \bar{\tau}_q + \sum_{p=1}^{n}\left(\vec{R}_{pq} + \dot{m}_{pq}\vec{u}_{pq}\right) + \alpha_q \rho_q \bar{F}_q \qquad \text{(Eq. 2)}$$

where, the terms on the left are the transient and convective terms. The terms on the right begin with pressure force followed by the shear force, the inter-phase force and the body forces.

and $\bar{\tau}_q$ is the q^{th} phase stress tensor where

$$\sum_{p=1}^{n} \vec{R}_{pq} = \sum_{p=1}^{n} K_{pq}(\vec{v}_p - \vec{v}_q) \qquad \text{(Eq. 2b)}$$

Conservation of energy for phase q :

To describe the conservation of energy in Eulerian multiphase model, a separate enthalpy equation can be written for each phase:

$$\frac{\partial}{\partial t}(\alpha_q \rho_q h_q) + \nabla \cdot (\alpha_q \rho_q \vec{u}_q h_q) = -\alpha_q \frac{dp_q}{dt} + \bar{\tau}_q . \nabla \vec{u}_q - \nabla \cdot \vec{q}_q + \sum_{p=1}^{n} \left(Q_{pq} + \dot{m}_{pq} h_{pq} \right) + S_q \qquad \text{(Eq. 3)}$$

where, the last three terms are respectively heat conduction, energy transfer with heat transfer and energy source term and h_q is the specific enthalpy of the q^{th} phase, $\vec{q}_q$ is the heat flux, S_q is a source term that includes sources of enthalpy (e.g., due to chemical reaction or radiation), Q_{pq} is the intensity of heat exchange between the p^{th} and q^{th} phases, and h_{pq} is the inter-phase enthalpy (e.g., the enthalpy of the vapor at the temperature of the droplets, in the case of evaporation) where:

$$Q_{pq} = h_{pq}(T_p - T_q) \qquad \text{(Eq. 3a)}$$

Bed thermochemical reaction sub-models

The biomass thermochemical conversion includes complex chemical and physical processes such as vaporization, devolatilization coupled with the bed flow hydrodynamics. Many studies have been performed and many models have been built to describe the process [8]

Devolatilization sub-models

The devolatilization process begins when the biomass temperature reaches a critical level, in this case assumed 300^0 C. Many biomass devolatilization models have been developed and several reviews of these models have been made [8]. The simplified approaches define devolatilization rates with a single-step Arrhenius reaction schemes. The one-step global mechanisms can be shown as:

$$BIOMASS \xrightarrow{k} \alpha_1 CHAR + \alpha_2 BIOIL + \alpha_3 H_2O + \alpha_4 CO + \alpha_5 CO_2 + \alpha_6 CH_4 \qquad \text{(Eq. 4)}$$

where α_i are the stoichiometric coefficients. The reaction kinetic rate k is expressed in single-step Arrhenius fashion as $k = (1-\alpha_q)A.\exp(-E_a / RT)$ and the devolatilization rate is

$$\frac{dm_p}{dt} = Ae^{-E/RT_p}(m_p - m_0) \qquad \text{(Eq. 5)}$$

$m \to m_0$ as $t \to \infty$ where m_0 and m_p is the initial and instantaneous mass of the biomass particle. The q^{th} phase void fraction is denoted by α_q.

During the pyrolysis process, the flux of gases leaving the particle prevents the previously formed gases (CO, H_2, CO_2 and CH_4) from approaching the surface of the reacting particle. To evaluate the seven unknown stoichiometric coefficients α_i, in equation (4), the appropriate representation of chemical formula for biomass, char and bio-oil are required. These were determined or calculated from the ultimate analysis data [9] such that the chemical formulae for palm fruit was assumed $CH_{0.98}O_{0.58}$. The chemical structure for bio-oil from palm fruit was assumed to be the same, i.e. $CH_{0.98}O_{0.58}$. Following the procedure in [9], the first coefficient α_1 is determined by assuming that the formed char equals the fixed carbon reported in the proximate analysis of the palm fruit [10]. From experimental data [9], the known ratios of CO/CO_2 and CH_4/CO provides additional information to solve for the six coefficients in equations (6a) through (6c).

Carbon balance:

$$1 = \alpha_1 + \alpha_2 + \alpha_3 + \alpha_6 + \alpha_7 \qquad \text{(Eq. 6a)}$$

Hydrogen balance:

$$0.98 = 0.98\alpha_2 + 2\alpha_3 + \alpha_4 + 4\alpha_7 \qquad \text{(Eq. 6b)}$$

Oxygen Balance:

$$0.58 = 0.58\alpha_2 + \alpha_3 + \alpha_5 + 2\alpha_6 \qquad \text{(Eq. 6c)}$$

The coefficients α_i were solved to predict the stoichiometric local composition and distribution of volatiles in the reactor and coupled in the CFD model by solving the transport equations 1 through 4 in the fluidized bed using FLUENT.

Results and discussion

The biomass reactor geometry is illustrated in Figure 1 depicting major sections of the reactor. The pyrolysis products from the reactor pass through series of cyclones (not shown) to separate the oil from the rest.

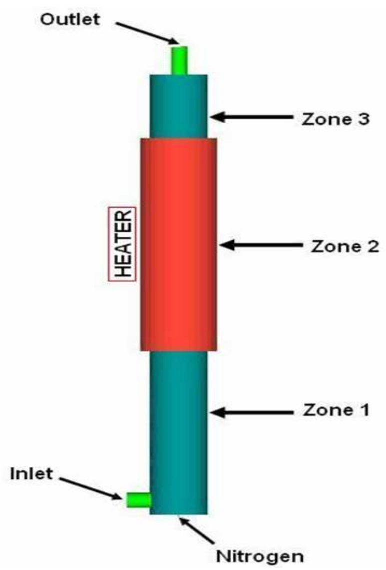

Figure 1: Fast pyrolysis biomass reactor [6]

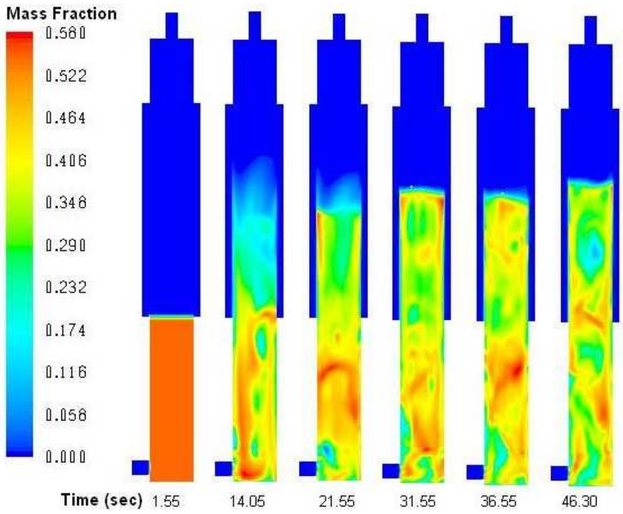

Figure 2: Distribution of sand in the reactor from static bed at 0 sec and expands steadily to fully expanded bed at 46.30 sec.

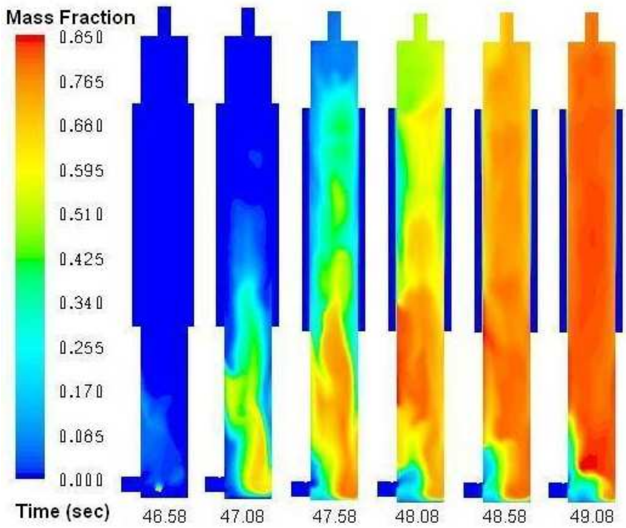

Figure 3: Contours depicting the distribution of bio-oil in the reactor during the pyrolysis process. It is observed that pyrolysis process commences at about 46.58 and proceeds fast to near completion within 3 seconds during which the reactor temperature is nearly uniform and corresponding to the time of maximum bed expansion.

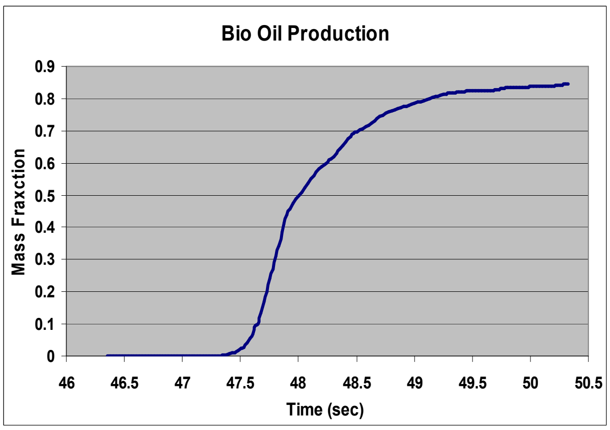

Figure 4: Bio-oil concentration at reactor the exit indicates the pyrolysis takes approximately 2 seconds to reach steady state at 50 seconds.

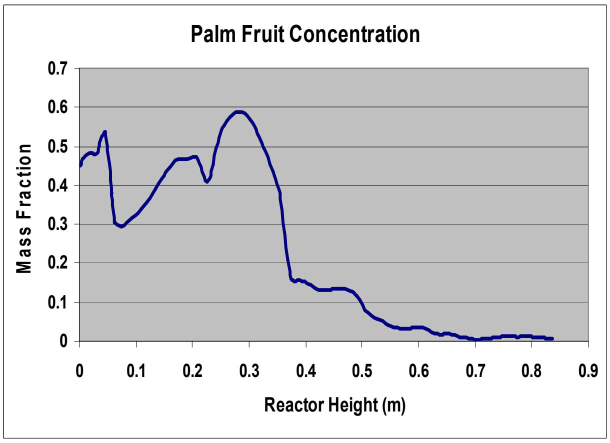

Figure 5: Concentration of biomass (palm fruit) along the axis of the reactor height indicates that most of the biomass is nearly consumed by mid height of the reactor

Conclusion

A model for predicting the simplified biomass pyrolysis and bio-oil yields has been presented. The formulation is based on reactor flow hydrodynamics and overall elemental balance supplemented by empirical correlations of ratios of different species. Model results indicate that nearly two-thirds of the reactor is actively producing bio-oil consistent with the widely reported in open literature. The model has been previously validated [11] against published experimental data on pyrolysis product composition for a typical biomass feedstock. Due to the complexity of biomass thermochemical conversion, a true generalized model must capture all the variability that might influence the fast pyrolysis product outcome. Nevertheless, the CFD technique may assist to optimize the design of the reactor for distributed farm scales. However, further work may be required to validate the model for different reactor operating conditions in addition to variety of biomass feedstock.

Acknowledgment: The author thanks A. A. Boateng for his collaboration in developing and validating the base CFD model for the biomass pyrolysis of switch grass and soy beans.

Nomenclature

A = pre-exponential constant.

m_p = mass of biomass particle (kg)

C_p = heat capacity of biomass (J/kg-K)

T_∞ = gas temperature inside gasifier (K)

H = sensible enthalpy (J/kg)

h = heat transfer coefficient (W/m^2 K)

ε = porosity

ε_p = emissivity of biomass particle

σ = Stefan-Boltzmann constant (W/m^{2}K^4)

θ_R = radiation temperature (K)

d_p = biomass particle diameter (m)

k_∞ = thermal conductivity gas phase (W/m-K)

R_e = Particle Reynolds number

$\Pr$ = Prandtl number of gas phase

R_m = moisture evaporation rate (kg/ m^3/s)

E_m = activation energy for drying (J/mol)

R = universal gas constant (J/mol-K)

T_m = gas phase temperature (K)

H_{fg} = biomass latent heat vaporization (J/kg)

E = activation energy (J)

T_p = temperature of biomass particle (K)

References

[1] S. Czernik and A. Bridgwater: V *Energy Fuels* 2004, *18*, 590–598.
[2] G. V. Huber, S. Iborra, A. Corma:. *Chem. Re*V. 2006, *106*, 4044–4098.
[3] D. M. Snider, P. J. O'Rourke and M. J. Andrews: Sediment Flow in Inclined Vessels Calculated Using Multiphase Particle-in-Cell Model for Dense Particle Flows, Int. J. Multiphase Flow, (1998) 24, 1359-1352
[4] C. C. Pain, S. Mansoorzadeh, J. L. M. Gomes, C. R. E. de Oliveira: A numerical investigation of bubbling gas–solid fluidized bed dynamics in 2-D geometries. Powder Technology 128 (1), (2002) 56–77.
[5] H. Gerhauser, S. C. Generalis, R. A. Hague A. V. Bridgwater: CFD for the Modeling of Entrainment in Fluidized Bed Fast Pyrolysis of Biomass; Progress in Thermochemical Biomass Conversion, (Blackwell, Oxford, UK 2001), pp. 1281-1295
[6] A. A. Boateng, D.E. Daugaard, N.M. Goldberg, K.B. Hicks: Bench-Scale fluidized bed pyrolysis of switch grass for bio-oil production; Ind. Eng. Chem. Res. 2007, 46, 1891-1897
[7] D. R. Gidaspow and J. Ding: Hydrodynamics of Circulating Fluidized Beds, Kinetic Theory Approach in Fluidization VII, Proceedings of the 7th, Engineering Foundation Conference on Fluidization, 75{82), 1992.
[8] C. D. Blasi: Modeling chemical and physical processes of wood and biomass pyrolysis. Progress in Energy and Combustion Science 2008, 34, 47-90.
[9] S. A. Mohamad: Pyrolysis of Empty Oil Palm Fruit Bunches Using the Quartz Fluidized- Fixed Bed Reactor MSc. Thesis (2008)
[10] T. B. Reed and B. A. Levie: A Simplified Model of the Stratified Downdraft Gasifer, Draft Report, Solar Energy Research Institute, Golden Colorado. (1983).
[11] A. A. Boateng and P. L. Mtui: CFD Modeling of space-time evolution of fast pyrolysis products in bench-scale fluidized bed reactor. Applied Thermal Engineering 33-34 (2012) 190-198